



Synthesis, Spectroscopic Characterization and Antimicrobial Studies of Mn(II), Co(II), Ni(II), Cr(III) and Fe(III) Melatonin Drug Complexes



Asma S. Al-Wasidi¹, Ahmed M. Naglah^{2,3}, Moamen S. Refat^{4,5}, Samy M. El-Megharbel^{4,6}, Atef Kalmouch³, Gaber O. Moustafa^{3,6*}

¹Department of Chemistry, College of Science, Princess Nourah Bint Abdulrahman University, Riyadh 11671, Saudi Arabia.

²Drug Exploration and Development Chair (DEDC), Department of Pharmaceutical Chemistry, College of Pharmacy, King Saud University, Riyadh 11451, Saudi Arabia,

³Peptide Chemistry Department, Chemical Industries Research Division, National Research Centre, 12622-Dokki, Cairo, Egypt.

⁴Department of Chemistry, Faculty of Science, Taif University, Al-Haweiah, 21974, Taif, Saudi Arabia.

⁵Department of Chemistry, Faculty of Science, Port Said University, Port Said, 42521, Egypt,

⁶Chemistry Department, Faculty of Science, Zagazig University, Zagazig 44519, Egypt.

⁶ Nahda University, New Benisuef City, Postal Code (62521), Beni Sueif, Egypt.

SYNTHESIS and characterizations of new Mn(II), Co(II), Ni(II), Cr(III) and Fe(III) melatonin drug complexes have been studied. The melatonin ligand act as a monodentate ligand through nitrogen of the deprotonated –NH pyrrole ring. This was confirmed by infrared spectra and microanalytical analysis. The magnetic moments data approved the complexity of Mn(II), Co(III), Ni(III) as a square planar and Cr(III), Fe(III) as an octahedral geometry, respectively. The biological activity of the melatonin free ligand is lower than that of the respected metal complexes. Thus, this indicates that the complexity is more effective than the antimicrobial activities of melatonin ligand.

Keywords: Melatonin drug, Synthesis, Antimicrobial, Complexes, Ligand.

Introduction

It has conclusively been shown that novel organic ligands are promising as biologically activate [1-21], melatonin is an organic ligand, N-acetyl-5-methoxy tryptamine (Fig.1), the principle hormone that is secreted from the pineal gland and it was isolated and characterized by Lerner et al. [22]. Melatonin is an indoleamine synthesized from L-tryptophan metabolism via serotonin [23]. Melatonin has potent antioxidant activities and a lot of therapeutic and prophylactic applications [24]. The melatonin reduction related to the aging series and may effect on life span [25]. Melatonin exogenous administration is very useful for treating circadian alterations, e.g., insomnia [26], jet lag [27]. Moreover, melatonin has pharmacological effects on the treatment of Alzheimer's disease [28], Parkinson disease [29],

glaucoma [30] depressive disorder [31] breast [32] and prostate cancer [33], hepatoma [34] and melanoma [35]. Unfortunately, a substitution therapy is not easily achieved with melatonin because of its relatively poor bioavailability [36] and rapid elimination [37]. Several methods for the determination of melatonin in biological fluids have been reported, such as enzyme immunoassay (EIA) [38], radioimmunoassay (RIA) [39], high-performance liquid chromatography with fluorescence [40-42] or electrochemical detection [43-45], capillary electrophoresis-ultraviolet detection (CE-UV) [46], gas chromatography–mass spectrometry (GC-MS/MS) [47-52].

Reactions of the melatonin with dipalmitoyl phosphatidylcholine multilamellar liposomes zwitterionic were expected as a reference of the temperature and the melatonin amount by

*Corresponding author; Email: gosman79@gmail.com, Tel. 00201003123355

Received 19/12/2019; Accepted 30/01/2020

DOI: 10.21608/ejchem.2020.21193.2263

©2020 National Information and Documentation Center (NIDOC)

two techniques, IR and differential scanning calorimetry [53]. The studies reveal that the physical properties of the DPPC bilayers changes by melatonin Asymmetric double bond vibrations. Furthermore, there are more than one spectrum is produced at large melatonin concentrations, which refers that melatonin-afforded a phase separation in the DPPC membranes.

The prevention of the lead toxicity is of a high international public health priority [54, 55]. The evaluation of the melatonin effects, the antioxidant and the free radical scavenging activities, on lead formed neurotoxicity and oxidative stress. Previous results suggested that melatonin treatment can improve the oxidative stress of impotence and disability by protecting the brain from lead toxicity. Due to the essential biological activities of this molecule, melatonin has been subjected of several structural and spectroscopic studies.

Melatonin and glutathione binding has been investigated by using the titration calorimetry and by using UV-vis absorption spectroscopy, Fourier transform infrared spectroscopy [56]. Thermodynamic investigations with addition of the daily doses of 0.2% $\text{Pb}(\text{CH}_3\text{COO})_2$ to drinking with the distilled water and continues till the weaning. Melatonin was administrated once daily, After 21 days, Multi antioxidant enzyme activities as superoxide dismutase and glutathione peroxidase were evaluated. Lipid peroxides levels were measured as a marker of lipid peroxidation confirmed that melatonin/ glutathione correlates to HSA which is driven by favorable entropy. The major forces are hydrogen bond and van der Waals. The interaction for glutathione is recognized by a high number of the binding sites, which informs that the binding takes place by adsorption surface which leads to the protein surface coating. Regarding the melatonin, one molecule of melatonin conjugates

with one molecule of HSA and no binding occurs between more melatonin with HSA in this study. The UV-vis analysis, IR, and spectroscopy suggested that melatonin and glutathione may afford a micro environmental changes of HAS. The experimental evidences suggested that the melatonin is responsible for influencing the diabetic complications [57] by reducing the unnecessary reactive oxygen production and protection of the beta cells, as they have low antioxidant capacity and normalize the oxidative status in the cells. Nitric oxide is known to induce a lot of nephrotic diseases that afforded by the lead toxicity and the current works have shown the role of the antioxidants in reducing the lead toxic effects. Melatonin is known for its direct and indirect antioxidant activities. Additionally, it is produced by natural way in mammals. Additionally, [58] reported that melatonin alleviates the lead toxic effects in the kidneys and with no alterations of NO metabolites. The synthesis of a new fluorescent coumarin-that containing analogues of melatonin was presented [59].

Nano system types, namely as lecithin/ chitosan nanoparticles and some types of chitosan micelles, have been prepared and characterized [60] for their potential in melatonin delivery, which is known to have hypotensive effect. The melatonin particle size and properties were studied as a function with presence of the nanosystem. Supplementations with melatonin are widely used in Europe and in the USA to attenuate delay of sleep disorders [61]. The European Commission approved mainly two health claims for the food that containing a melatonin. The method of determination of melatonin dose in food that was marketed in Europe by confirming a liquidchromatography with diode array detection method. Contaminants that are present in melatonin supplements were estimated by using high- liquid performance chromatography and mass spectrometer.

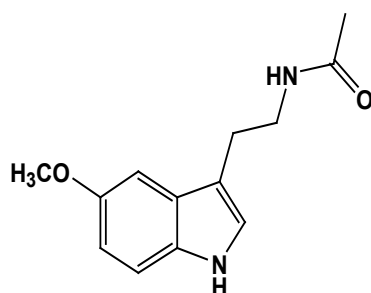


Fig. 1. Melatonin structure.

Experimental

Chemicals, reagents and instrumentals

The chemicals that were used from (Merck which is the high purest grade. The drug melatonin was purchased from The Egyptian Pharmaceutical Company (EIPICO). C and H amounts were detected using a Perkin-Elmer. The metal amount was measured by converting the complexity into their analogous stable oxide forms. Infrared spectra were estimated by Bruker FT-IR spectrophotometer (ranged from 4000–400 cm^{-1}) in KBr pellets. Molar conductivities of freshly prepared DMSO solutions were estimated by using Jenway. The X-ray diffraction patterns for the solid complexes were recorded on X'Pert PRO PANalytical X-ray powder diffraction, target copper with secondary monochromate. Scanning electron microscopy (SEM) images were taken in Quanta FEG 250 equipment. The mass susceptibility (X_g) of the solid paramagnetic Chromium(III), Manganese (II), Iron(III), Cobalt(II), and Nickel(II) complexity was detected using Gouy's method at the room temperature by using a magnetic balance at central lab at Cairo university. The effective magnetic moment (μ_{eff}) values were obtained by using the following equations (1, 2 and 3) [62].

$$X_g = \frac{C_{\text{Bal}} L (R - R_0)}{10^9 M} \dots \dots \dots (1)$$

Where:

R_0 = Empty tube reading

L = Length of the sample (cm)

M = Mass of the sample (gm)

R = The reading for tubes with samples

C_{Bal} = Constant of calibration balance = 2.086

$X_M = X_g \times M \cdot \text{Wt} \dots \dots \dots (2)$

The amounts of X_M were estimated from equation (2) and were corrected by using the Pascal's constants, and were applied in the Curie's equation (3).

$$\mu_{\text{eff}} = 2.84 \sqrt{X_M \times T} \dots \dots \dots (3)$$

Where T = t ($^{\circ}\text{C}$) + 273

Thermogravimetric Analysis (TGA) and Differential Thermal Analysis (DTA) were estimated by special thermal analyzers at Cairo university. All the experiments were carried out by a single loose top loading platinum sample pan under N_2 atmosphere at a flow level of 30 ml/min and a $10^{\circ}\text{C}/\text{min}$ with using temperature range 25–800 $^{\circ}\text{C}$

Antibacterial and anti-fungal evaluation

Regarding Gupta et al., [63] hole-well methods

that were applied. The examined bacterial isolates were seeded in tubes with the nutrient media. The seeded NB was homogenized with the melted agar media. The suspensions were poured in the Petri dishes. The inhibition zone diameter that was over than 7 mm indicated that the tested compounds were active against the bacterial activity. The antibacterial activities were tested against *Escherichia coli*, *Bacillus subtilis* and anti-fungal (*Aspergillus oryzae*, *niger* and *Flavus*).

Synthesis of melatonin complexes

The Chromium(III), Manganese (II), Iron(III), Cobalt(II), and Nickel(II) complexity were synthesized by reactions CrCl_3 , $\text{MnCl}_2 \cdot 4\text{H}_2\text{O}$, $\text{FeCl}_3 \cdot 2\text{H}_2\text{O}$, $\text{CoCl}_2 \cdot 6\text{H}_2\text{O}$ and $\text{NiCl}_2 \cdot 6\text{H}_2\text{O}$ metals (1 mmol; 20 mL distilled water) to melatonin (2 mmol; 20 ml 99% Methanol) with molar ratio 1:2 for all complexity except Cr(III) and Fe(III) is 1:3 ratio. Concentration of hydrogen for melatonin metal ions complexity were adjusted between 7–9 by using 5% Ammonium hydroxide/Methanol. The obtained solutions were stirred and refluxed on a hot plate at 60 $^{\circ}\text{C}$ for about 1 h. The products were taken, filtered and were washed with mixing of the distilled water with CH_3OH then were dried at 70 $^{\circ}\text{C}$ and remains under vacuum over the anhydrous CaCl_2 .

Results and Discussions

Physical properties

MLT ligand physical data and their complexity with Chromium(III), Manganese (II), Iron(III), Cobalt(II), and Nickel(II) are in Table 1. The product complexity are stable in the air, and with high melting points. Water and most organic solvents insoluble except in DMSO and in DMF. The ligand character of MLT with some metal ions were investigated by the infrared spectra, thermogravimetric analyses and molar conductance. The measuring of (C,H,N) of the complexity show 1:2 or 1:3 (metal: MLT) stoichiometry for Manganese (II), Cobalt(II), Nickel(II) (Chromium(III) and Iron(III)) complexity, respectively. The amount of μ_{eff} were detected at room temperature for Manganese(II), Cobalt(II), Nickel(II), Chromium(III) and Iron(III) MLT complexity and have paramagnetic characters. The molar conductance data of the complexity which is low refers to non-electrolytic nature [64]; this proves the suggestion for Cl anions absence with no covalently bonded with the metal ions. This is in a complete agreement with the isolated complexes elemental analysis. The data obtained are in convenient with the expected structures (Fig. 2): $[\text{Cr}(\text{MLT})_3(\text{H}_2\text{O})_3] \cdot \text{H}_2\text{O}$, $[\text{Mn}(\text{MLT})_2(\text{H}_2\text{O})_2]$, $[\text{Fe}(\text{MLT})_3(\text{H}_2\text{O})_3] \cdot \text{H}_2\text{O}$, $[\text{Co}(\text{MLT})_2(\text{H}_2\text{O})_2] \cdot 2\text{H}_2\text{O}$, $[\text{Ni}(\text{MLT})_2(\text{H}_2\text{O})_2] \cdot 2\text{H}_2\text{O}$.

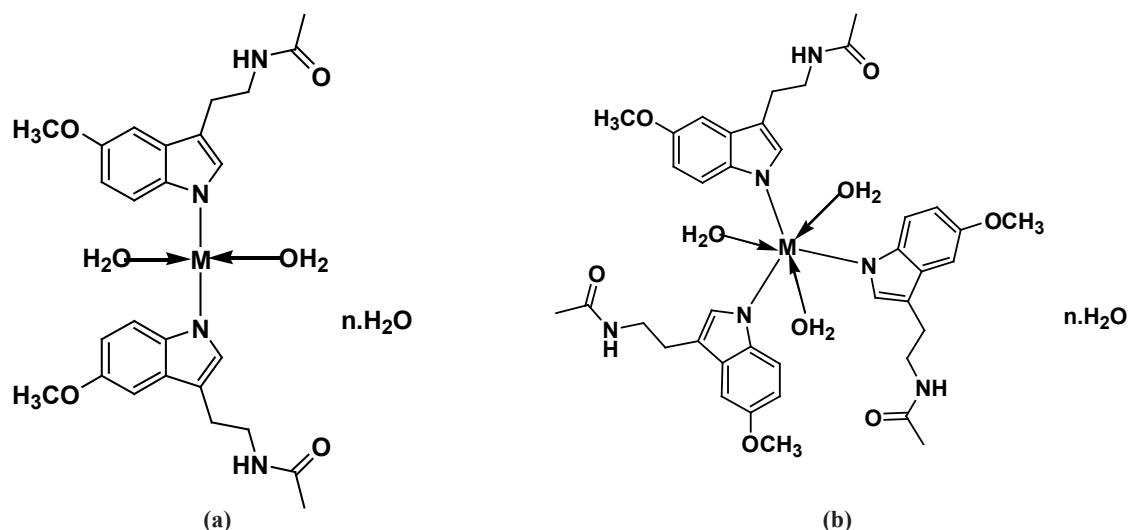


Fig. 2. The mode of coordination of M(II) / Melatonin complexes where (M = Mn, Co and Ni & n= 0, 2 and 2 respectively); (2b): The mode of coordination of M(III)/Melatonin complexes where (M= Cr and Fe).

TABLE 1. Physicochemical data of MLT metal complexes.

Empirical formula	Color	Mwt.	Am (μ S)	Elemental analysis, % Found % (Calcd.)			
				C	H	N	M
[Cr(MLT) ₃ (H ₂ O)].H ₂ O	greenish	817	28	57.35 (57.28)	6.91 (6.48)	10.19 (10.28)	5.98 (6.36)
[Mn(MLT) ₂ (H ₂ O) ₂]	brown	553	25	56.87 (56.48)	6.52 (6.14)	9.87 (10.12)	9.78 (9.94)
[Fe(MLT) ₃ (H ₂ O) ₃].H ₂ O	Dark green	821	26	57.31 (57.00)	6.73 (6.45)	9.96 (10.23)	6.73 (6.82)
[Co(MLT) ₂ (H ₂ O) ₂].2H ₂ O	brown	593	24	52.85 (52.64)	6.72 (6.40)	9.32 (9.44)	9.87 (9.94)
[Ni(MLT) ₂ (H ₂ O) ₂].2H ₂ O	Faint green	593	24	52.52 (52.64)	6.60 (6.41)	9.64 (9.44)	9.89 (10.07)

Infrared spectra

IR spectra of melatonin and its complexity were measured in Fig. 3 and Table 2. The IR spectra of melatonin complexity are correlated; this is may be due to the coordination site toward Cr(III), Mn(II), Fe(III), Co(II) and Ni(II) ions which are the same. The most importance property of the IR spectra of the complexity is the disappearance of aband at 3360cm⁻¹. The strong band at 3360cm⁻¹ assigned to NH (indole) disappear in complexes which may be attributed to formation o nitrogen-metal band However, MLT has two spectra at 3360, and 3300 cm⁻¹. This

fact is difficult to reconcile with the proposed structures by Fazakerley *et al.* [65]. Strong bands at 3300 cm⁻¹ can be attributed to NH (amide) which is not affected; this indicates that the NH group is not participated in the coordination mechanism. Spectrum at 1621 cm⁻¹, due to C=O stretching vibration, is not affected in the complexity and has low intensity. Spectra at 1315 and 1214 cm⁻¹ in MLT do not shift in complexity. Nakamoto [66] attributed to the spectra at 1315 and 1214 cm⁻¹ in the metal oxamido complexes to the Carbon-Nitrogen vibration. If we consider that the 1315 and 1214 cm⁻¹ bands were due to

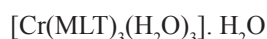
C-N vibration, we deduce that the NHCO group was not participated in coordination process. The free MLT has a band in C-O region, at 1170 cm^{-1} . After the complexity, the maxima is the same without changes, we conclude that the C-O association probably did not share the complexity, the presence of a medium to weak bands at (523-622) cm^{-1} can be owned to Metal-Nitrogen stretching vibration motion [67].

Magnetic measurements

Magnetic measurements were obtained by Gouy method [72] and the observed values for the iron(III) and chromium(III) complexes are 5.26 and 3.64 BM in the accepted scale with an octahedral geometry [68, 69]. The Mn(II) complex shows a magnetic moment (5.92 B.M) which are appreciably close to the calculated spin-only value for five unpaired electrons, and reveal a high spin state, therefore, the structure of the prepared Mn(II) complex. This indicates a square planer geometry around Mn(II) ion [70, 71]. The magnetic data of the $[\text{Co}(\text{MLT})_2(\text{H}_2\text{O})_2] \cdot 2\text{H}_2\text{O}$ complex is agreement with that reported for related cobalt(II) complexes [70]. This geometry is confirmed by the values of the effective magnetic moment (1.81 BM) suggests a square-planar geometry. The square planar Ni (II) complexes are a diamagnetic (0.0 B.M.) meanwhile, the tetrahedral complexes have moments in (3.20–4.10 B.M), and octahedral complexes should have moments between 2.90–3.30 B.M. [72-74]. The Ni(II) complex gave a moment of 0.0 B.M. and hence attributed as a square planer.

Thermal analysis of MLT complexes

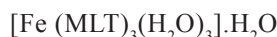
The thermo gravimetric analysis occurs at 10°C/min at N_2 atmosphere. The weight loss was measured upto 136 °C. The thermal products are shown in Table 3 and shown in Fig. 4. The losses in weight for each complexity were estimated in the ranges of the correlating temperatures.



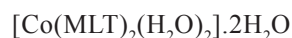
The thermal degradation of $[\text{Cr}(\text{MLT})_3(\text{H}_2\text{O})_2] \cdot \text{H}_2\text{O}$ complex takes place at 3 steps. The 1st decomposition step occurs in temperature range (50-230°C) and this refers to the loss of (H_2O), weight loss (Obs.=2.46%, calc = 2.20%). The 2nd step occurs (230-417°C) that is attributed to the $3\text{H}_2\text{O} + \text{C}_{18}\text{H}_{25}\text{O}_2$ loss (Organic moiety) (obs. = 40.06%, calc= 40.02%). The last degradation step takes place at temperature range 430-490°C, while the weight loss is (Obs.=48.32% ,calc= 48.47%), which are attributed to $\text{C}_{21}\text{H}_{20}\text{N}_6\text{O}_{1.5}$ loss. The last residue $\text{CrO}_{1.5}$ remains stable till 800 °C.



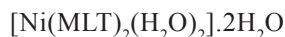
The Mn(II) complex is degraded in 2 steps. The 1st step is occurred at 50-300°C and corresponding to the loss of $2\text{H}_2\text{O} + \text{C}_{18}\text{H}_{22}\text{O}_2$ (Organic moiety) (obs. = 55.06%, calc. = 55.33%). The 2nd step occurs in the range (300–500°C) and can be attributed due to $\text{C}_7\text{H}_8\text{N}_4\text{O}$ loss (obs. = 52.02%, calc. = 52.34%). The last residue was produced at 800°C is $\text{MnO} + \text{C}$.



Fe (III) complex decomposed thermally at 4 steps. The 1st step occurs in (40-80 °C) and they were attributed to the loss of 1.5 H_2O molecule (obs. = 3.20%, calc. = 3.28%). The 2nd step is (80-160 °C) which is attributed to the loss of 2.5 H_2O with a weight loss (obs. = 5.79%, calc. = 5.48%). The 3rd step occurs within the temperature (160-280°C) can be assigned to loss $\text{C}_{18}\text{H}_3\text{O}_3\text{N}_3$ with representing weight loss (obs. = 35.84%, calc. = 35.08%). The last degradation step in (280-450 °C) is joined by (calc. = 28.86%), which are attributed to the loss of $\text{C}_9\text{H}_{15}\text{N}_3\text{O}_{4.5}$. The $\text{FeO}1\frac{1}{2} + 12\text{C}$ are the last product that remains stable till the temperature 800 °C.



Cobalt complexity is degraded in 3 steps. The 1st step was obtained at 50-100°C and was corresponding to 4(H_2O) molecules evolution, that represent (Obs=12.31%, Calc= 12.14%). While, the 2nd decomposition step is carried out at 100-277°C and attributed to the loss of $\text{C}_6\text{H}_{10}\text{N}_3\text{O}$ (Obs= 23.61%, Calc=23.60%). The last degradation step takes at 277-490°C and was attributed to $\text{C}_{11}\text{H}_{20}\text{NO}_2$ loss with (Obs= 33.62% and Calc= 33.89%). The residue resulted at 800°C which is CoO.



Ni(II) compound is degraded in 3 steps. The 1st step is carried out at 50-105°C and refers to 4(H_2O) loss, that represent the weight loss as follows (obs. =12.17%, calc= 12.14%). The 2nd step occurs in (105-280°C) and can be attributed to $\text{C}_6\text{H}_{10}\text{N}_3\text{O}$ loss with (obs. = 23.58%, calc =23.62%). The last step is occurring at (280-500 °C) and attributed to $\text{C}_{11}\text{H}_{20}\text{NO}_2$ loss that represent a weight loss of 33.12 %, (Calc= 33.40%). The final residues were obtained at 800°C are $\text{NiO} + 9\text{C}$

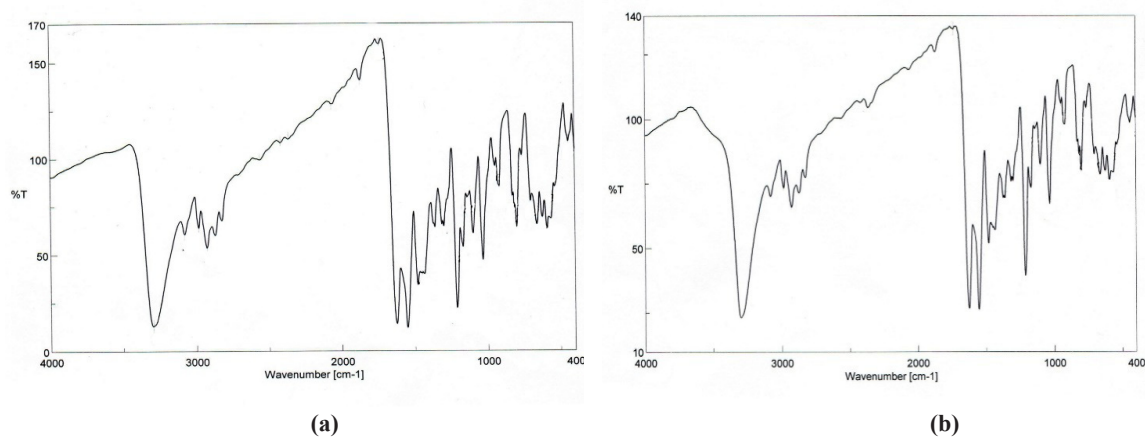


Fig. (3a). IR of Mn /MLT complex; (3b): IR of Fe /MLT complex.

TABLE 2. Infrared spectral bands and assignments of (MLT) complexes.

Compound	$\nu(\text{N-H})$ Indole	$\nu(\text{N-H})$ amide	$\nu(\text{C=O})$ amide	$\nu(\text{C-N})$	$\nu(\text{C-O})$	$\nu(\text{M-N})$
MLT	3360	3300	1620	1315, 1213	1170	-----
Cr	-----	3298	1622	1315, 1213	1171	621, 592, 564
Mn	-----	3299	1621	1315, 1213	1170	622, 592, 564
Fe	-----	3298	1622	1315, 1213	1171	622, 592, 539
Co	-----	3299	1623	1315, 1213	1171	626, 593, 523
Ni	-----	3297	1621	1315, 1213	1172	626, 590

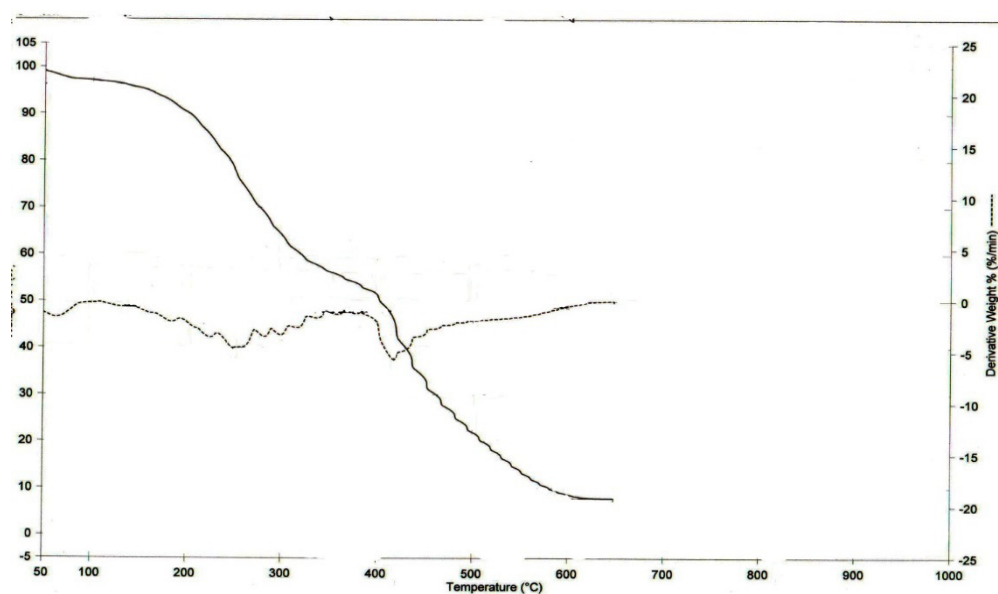


Fig. 4. TG/DTG of Cr /MLT complex.

TABLE 3. Thermogravimetric data of the MLT complexes.

Compound	Steps	DTG peak (°C)	TG Weight loss (%)		Assignments
			Calc.	Found	
Cr(III)	1 st	230	2.2	2.46	-H ₂ O
	2 nd	417	40.02	40.06	-3H ₂ O+C ₁₈ H ₂₅ O ₂
	3 rd	490	48.47	48.32	-C ₂₁ H ₂₀ N ₆ O _{2.5} residue(CrO _{1.5})
Mn(II)	1 st	300	55.33	55.06	-2H ₂ O+C ₁₈ H ₂₂ O ₂
	2 nd	500	29.65	30.08	-C ₇ H ₈ N ₄ O residue(MnO+C)
Fe(III)	1 st	80	3.28	3.20	-1.5H ₂ O
	2 nd	160	5.48	5.79	-2.5H ₂ O
	3 rd	280	35.08	35.84	-C ₁₈ H ₃₀ N ₃
	4 th	450	28.86	28.90	-C ₉ H ₁₅ N ₃ O _{4.5} residue(FeO _{1.5} +12C)
Co(II)	1 st	100	12.14	12.31	-4H ₂ O
	2 nd	277	23.60	23.61	-C ₆ H ₁₀ N ₃ O
	3 rd	490	33.89	33.62	-C ₁₁ H ₂₀ NO ₂ residue(CoO)
Ni(II)	1 st	105	12.14	12.17	-4H ₂ O
	2 nd	280	23.62	23.58	-C ₆ H ₁₀ N ₃ O
	3 rd	500	33.40	33.12	-C ₁₁ H ₂₀ NO ₂ residue(NiO+9C)

XRD and SEM investigations

XRD and SEM analysis showed the crystalline nature of the metal complexes. The samples of melatonin solid complexes were characterized at the room temperature by the X-ray diffraction by using the Cu K α radiation. The X-ray diffraction patterns of the synthesized MLT complexes are crystalline in nature. The diffraction characterization of the synthesized MLT complexes recorded in between 4° to 90°. The crystalline size of synthesized complexes is calculated using the Scherrer formula [63] $D = kl/b\cos\theta$, where k is a constant and equal 0.94, l the wavelength of X-ray used (0.154 nm) and b is a full in width at half maxima peak of XRD pattern. The crystalline size was found for cobalt and nickel complexes 50 nm and 30 nm, respectively. It is observed that crystalline size is different for both the complexes, due to change in the metal ions. The XRD patterns are shown in Fig. 5.

The SEM image of the MLT complexes are shown in Fig. 6. From this figure, it can be seen that the average length of the grains for the cobalt(II) and nickel(II) complexes are 50-100 μm , respectively. The surface morphology changes with change in metal ions, both the images having large number of irregular shaped

and some having regular grains.

Antimicrobial activity

As shown in (Fig 5 and Table 4), The antimicrobial activities were elevated in this order: Mn⁺²\MLT(1.10-2.70 cm) > Fe⁺³\ MLT(1.50-2.50 cm)> Ni⁺²\ MLT(1.00-2.00 cm)> Co⁺²\MLT (0.50-1.50 cm) >Cr⁺³\ MLT(1.00-1.30 cm).Cr⁺³\ MLT was the least active being active against five bacteria and fungi, Escherichia coli (Gram-ve), Bacillus subtilis (Gram +ve) and anti-fungal (*Aspergillus oryzae*, *niger*, *Flavus*). The high MLT complexes sensitivity have been assigned to hyper-conjugation of the coordinated Lewis bases, which elevates all the electrons density on the metal ions coordinated form with highest antimicrobial activity [64].

Acknowledgements

This Research was funded by The Deanship of Scientific Research at Princess Nourah Bint Abdulrahman University through the Fast-Track Research Funding Program.

Conflict of Interest

The authors declare no potential conflicts of interest with respect to the research, authorship, and publication of this article.

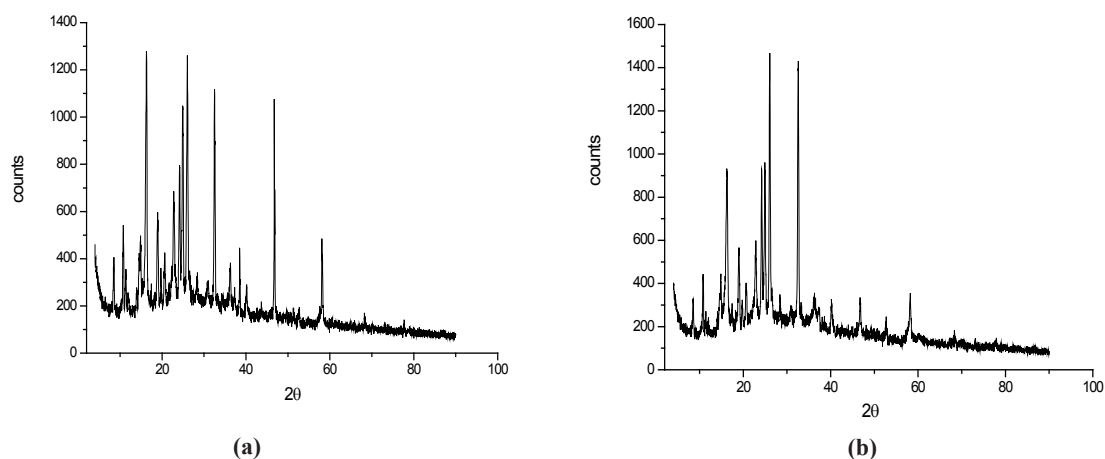


Fig. 5. XRD spectrum of Co(II) complex; (b) XRD spectrum of Ni(II) complex.

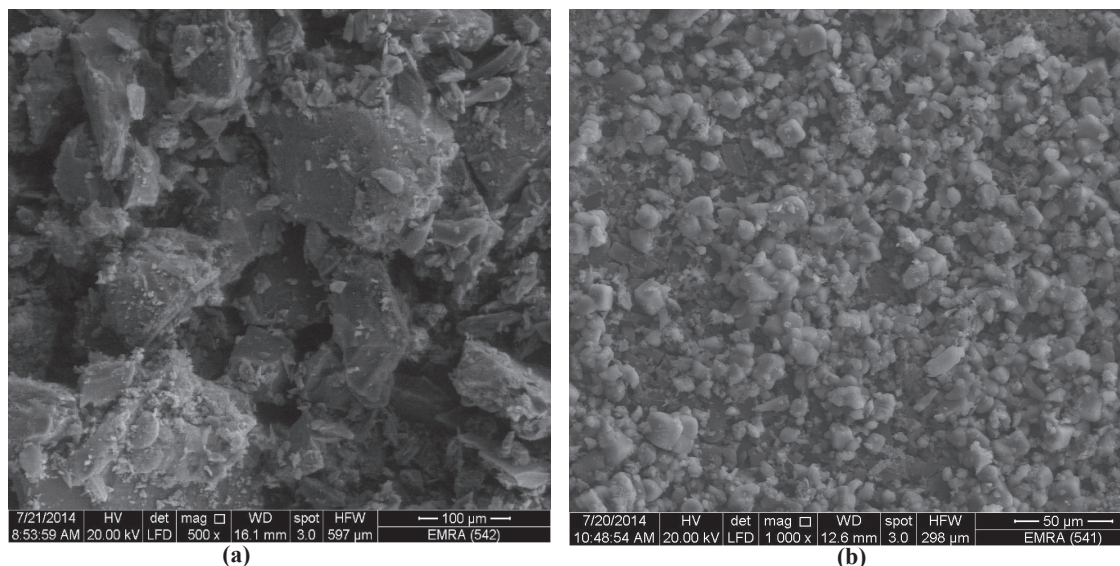


Fig. 6. SEM spectrum of Co(II) complex; (b) SEM spectrum of Ni(II) complex.

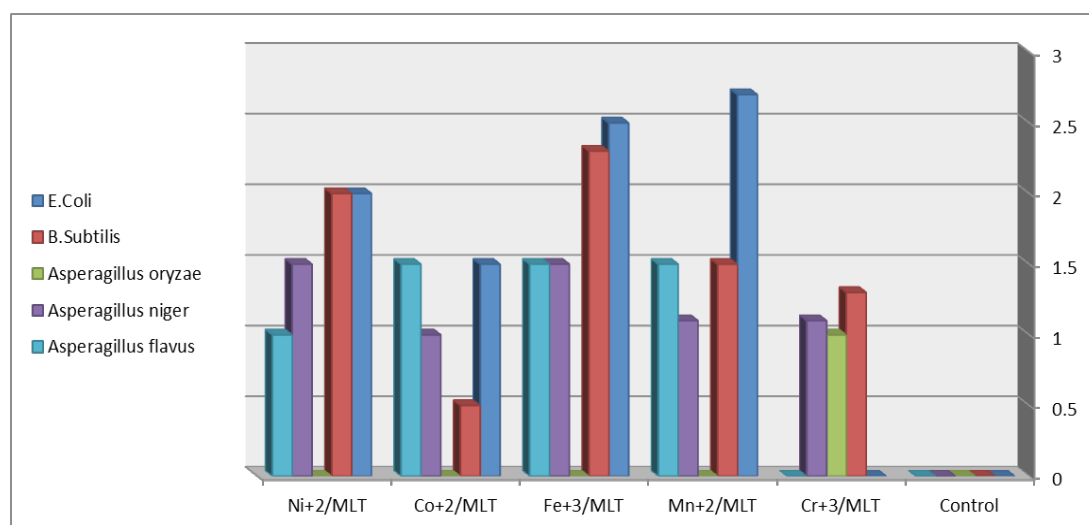


Fig. 7. Inhibition zone diameter (mm/mg) sample of DMSO (Control) and MLT complexes.

TABLE 4. The inhibition zone diameter (mm/mg sample) of complexes against some kind of bacteria and fungi.

Complexes	Diameter of inhibition zone (Cm)				
	<i>E.Coli</i>	<i>B.subtilis</i>	<i>Asperagillus oryzae</i>	<i>Asperagillus niger</i>	<i>Asperagillus Flavus</i>
Control	0.0	0.0	0.0	0.0	0.0
Cr ⁺³ \MLT	0.0	1.3	1.0	1.1	0.0
Mn ⁺² \MLT	2.7	1.5	0.0	1.1	1.5
Fe ⁺³ \MLT	2.5	2.3	0.0	1.5	1.5
Co ⁺² \MLT	1.5	0.5	0.0	1.0	1.5
Ni ⁺² \MLT	2.0	2.0	0.0	1.5	1.0

References

- Moustafa G.O., El-Sawy A.A. and Abo-Ghalia M.H., Synthesis of Novel Cyclopeptide Candidates: I-Cyclo-[N⁶-isophthaloyl-bis-(Glycine-Amino Acid)-L-Lysine] Derivatives with Expected Anticancer Activity., *Egypt. J. Chem.*, **56**(5), 473-494 (2013).
- Abo-Ghalia M.H., Moustafa G.O., Alwasidi A.S. and Naglah A.M., Cytotoxic investigation of isophthaloyl cyclopentapeptides., *Lat. Am. J. Pharm.*, **36**(10), 1957-1962 (2017).
- Amr A.E.E., Abo-Ghalia M.H., Moustafa G.O., Al-Omar M.A., Nossier E.S. and Elsayed E.A., Design, synthesis and docking studies of novel macrocyclic pentapeptides as anticancer multi-targeted kinase inhibitors., *Molecules*, **23**, 2416 (2018).
- Moustafa G.O., Younis A., Al-Yousef S.A. and Mahmoud S.Y., Design, synthesis of novel cyclic pentapeptide derivatives based on 1, 2-benzenedicarbonyl chloride with expected anticancer activity., *J. Comput. Theor. Nanosci.*, **16**(5-6), 1733-1739 (2019).
- Kassem A.F., Moustafa G.O., Nossier E.S., Khalaf H.S., Mounier M.M., Al-Yousef S.A. and Mahmoud S.Y., In vitro anticancer potentiality and molecular modelling study of novel amino acid derivatives based on N¹, N³-bis-(1-hydrazinyl-1-oxopropan-2-yl) isophthalamide., *J. Enzyme Inhib. Med. Chem.*, **34**(1), 1247-1258 (2019).
- Elhenawy A.A., Al-Harbi L.M., Moustafa G.O., El-Gazzar M.A., Abdel-Rahman R.F. and Salim A.E., Synthesis, comparative docking, and pharmacological activity of naproxen amino acid derivatives as possible anti-inflammatory and analgesic agents., *Drug Des. Devel. Ther.*, **13**, 1773-1790 (2019).
- Naglah A.M., Moustafa G.O., Al-Omar M.A., Al-Salem H.S.A. and Hozzein W.N., Synthesis, characterization and in vitro antimicrobial investigation of novel amino acids and dipeptides based on dibenzofuran-2-sulfonyl-chloride., *J. Comput. Theor. Nanosci.*, **14**(7), 3183-3190 (2017).
- Al-Salem H.S.A., Naglah A.M., Moustafa G.O., Mahmoud A.Z. and Al-Omar M.A., Synthesis of novel tripeptides based on dibenzofuran-2-sulfonyl-[aromatic and hydroxy aromatic residues]: Towards antimicrobial and antifungal agents., *J. Comput. Theor. Nanosci.*, **14**(8), 3958-3966 (2017).
- Moustafa G.O., Khalaf H., Naglah A., Al-Wasidi A., Al-Jafshar N. and Awad H., The Synthesis of Molecular Docking Studies, In Vitro Antimicrobial and Antifungal Activities of Novel Dipeptide Derivatives Based on N-(2-(2-Hydrazinyl-2-oxoethylamino)-2-oxoethyl)-nicotinamide., *Molecules*, **23**(4), 1-13 (2018).
- Mohamed F.H., Shalaby A.M., Soliman H.A., Abdelazem A.Z., Mounier M.M., Nossier E.S. and Moustafa G.O., Design, Synthesis and Molecular Docking Studies of Novel Cyclic Pentapeptides Based on Phthaloyl Chloride with Expected Anticancer Activity. *Egypt. J. Chem.*, **63**(5) (2020).
- Hasanin, M.S., Moustafa, G.O. New potential green, bioactive and antimicrobial nanocomposites based on cellulose and amino acid. *International Journal of Biological Macromolecules*, **144**, 441-448 (2019).

12. Elsherif, M.A., Hassan, A.S., Moustafa, G.O., Awad, H.M., Morsy, N.M. Antimicrobial Evaluation and Molecular Properties Prediction of Pyrazolines Incorporating Benzofuran and Pyrazole Moieties. *Bulletin of the Chemical Society of Ethiopia*, **10** (02), 037-043 (2020).
13. Asma S. Al-Wasidi, Ahmed M. Naglah, Atef Kalmouch, Abdel Majid A. Adam, Moamen S. Refat, Gaber O. Moustafa, Preparation of Cr₂O₃, MnO₂, Fe₂O₃, NiO, CuO, and ZnO Oxides Using Their Glycine Complexes as Precursors for In Situ Thermal Decomposition. *Egypt. J. Chem.*, **63** (3), 1109-1118 (2020).
14. Asma S. Al-Wasidi, Mohamed Wafeek, Haytham A. Abd El-Ghaffar, Ahmed M. Naglah, Atef Kalmouch, Mona Hamed, Gaber O. Moustafa, Effect of Density on Growth Hormone and Some Physiological Parameters and its Relation to Growth Performance. *Egypt. J. Chem.*, **63** (4), 1571-1580, (2020).
15. Moustafa, G.O., Al-Wasidi, A.S., Naglah, A.M., Refat, M.S. Isolation and Synthesis of Dibenzofuran Derivatives Possessing Anticancer Activities: A Review. *Egypt. J. Chem.*, **63** (6), in press, (2020).
16. Abo-Ghalia, M.H., Moustafa, G.O., Amr, A.E., Naglah, A.M., Elsayed, E.A., Bakheit, A.H. Anticancer activities and 3D-QSAR studies of some new synthesized macrocyclic heptapeptide derivatives. *Molecules*, **25** (5), 1253 (2020).
17. Kalmouch, A., Radwan, M.A.A., Omran, M.M., Sharaky, M., Moustafa, G.O. Synthesis of novel 2, 3'-bipyrrrole derivatives from chalcone and amino acids as antitumor agents. *Egypt. J. Chem.* **63**, (2020), in press.
18. Hassan, A.S., Moustafa, G.O., Awad, H.M. Synthesis and in vitro anticancer activity of pyrazolo [1, 5-a] pyrimidines and pyrazolo [3, 4-d] [1, 2, 3] triazines. *Synth. Commun.* **47**, 1963-1972 (2017).
19. Hassan, A.S., Moustafa, G.O., Askar, A.A., Naglah, A.M., Al-Omar, M.A. Synthesis and antibacterial evaluation of fused pyrazoles and Schiff bases. *Synthetic Communications*, **48**, 2761-2772, (2018).
20. Hassan, A.S., Moustafa, G.O., Morsy, N.M., Abdou, A.M., Hafez, T.S. Design, synthesis and antibacterial activity of N-aryl-3-(arylamino)-5-(((5-substituted furan-2-yl) methylene) amino)-1H-pyrazole-4-carboxamide as Nitrofurantoin® analogues. *Egypt. J. Chem.*, **63**, (2020) in press.
21. Hassan, A.S., Askar, A.A., Nossier, E.S., Naglah, A.M., Moustafa, G.O., Al-Omar, M.A. Antibacterial Evaluation, In Silico Characters and Molecular Docking of Schiff Bases Derived from 5-aminopyrazoles. *Molecules*. **24**(17), 3130 (2019).
22. Lerner AB, Case JD, Takahashi Y, Lee TH, Mori W. Isolation of melatonin, the pineal gland factor that lightens melanocyteS1. *Journal of the American Chemical Society* **80**, 2587 (1958).
23. Reiter RJ. Pineal melatonin: cell biology of its synthesis and of its physiological interactions. *Endocrine reviews* **12**, 151-80 (1991).
24. Livrea MA, Tesoriere L, D'Arpa D, Morreale M. Reaction of melatonin with lipoperoxyl radicals in phospholipid bilayers. *Free Radical Biology and Medicine* **23**, 706-111 (1997).
25. Bubenik G, Konturek S. Melatonin and aging: prospects for human treatment. *Journal of physiology and pharmacology* **62**, 13 (2011).
26. Jan JE, Reiter RJ, Wasdell MB, Bax M. The role of the thalamus in sleep, pineal melatonin production, and circadian rhythm sleep disorders. *Journal of pineal Research* **46**, 1-7 (2009).
27. Zhou JN, Liu RY, Kamphorst W, Hofman MA, Swaab DF. Early neuropathological Alzheimer's changes in aged individuals are accompanied by decreased cerebrospinal fluid melatonin levels. *Journal of pineal research* **35**, 125-130 (2003).
28. Adi N, Mash DC, Ali Y, Singer C, Shehadeh L, Papapetropoulos S. Melatonin MT1 and MT2 receptor expression in Parkinson's disease. *Medical science monitor* **16**, BR61-BR7 (2010).
29. Lundmark PO, Pandi-Perumal SR, Srinivasan V, Cardinali DP. Role of melatonin in the eye and ocular dysfunctions. *Visual neuroscience* **23**, 853-862 (2006).
30. Dubocovich ML. Melatonin is a potent modulator of dopamine release in the retina. *Nature* **306**, 782 (1983)
31. Tamarkin L, Danforth D, Lichter A, DeMoss E, Cohen M, Chabner B, et al. Decreased nocturnal plasma melatonin peak in patients with estrogen receptor positive breast cancer. *Science* **216**, 1003-1005 (1982).
32. Xi SC, Siu SW, Fong SW, Shiu SY. Inhibition

- of androgen-sensitive LNCaP prostate cancer growth in vivo by melatonin: association of antiproliferative action of the pineal hormone with mt1 receptor protein expression. *The Prostate* **46**, 52-61 (2001).
33. Blask DE, Sauer LA, Dauchy RT, Holowachuk EW, Ruhoff MS, Kopff HS. Melatonin inhibition of cancer growth in vivo involves suppression of tumor fatty acid metabolism via melatonin receptor-mediated signal transduction events. *Cancer research* **59**, 4693-4701 (1999).
34. Slominski A, Pisarchik A, Semak I, Sweatman T, Wortsman J, Szczesniewski A, Serotonergic and melatonergic systems are fully expressed in human skin. *The FASEB journal* **16**, 896-898 (2002).
35. DeMuro RL, Nafziger AN, Blask DE, Menhinick AM, Bertino Jr JS. The absolute bioavailability of oral melatonin. *The Journal of Clinical Pharmacology* **40**, 781-874 (2000).
36. Claustrat B, Brun J, Chazot G. The basic physiology and pathophysiology of melatonin. *Sleep medicine reviews* **9**, 11-24 (2005).
37. Ferrua B, Masseyeff R. Immunoassay of melatonin with enzyme-labeled antibodies. *Journal of immunoassay* **6**, 79-94 (1985).
38. Arendt J, Paunier L, Sizonenko PC. MELATONIN RADIOIMMUNOASSAY. *The Journal of Clinical Endocrinology & Metabolism* **40**, 347-350 (1975).
39. Mills MH, King MG, Keats NG, McDonald RA. Melatonin determination in human urine by high-performance liquid chromatography with fluorescence detection. *Journal of Chromatography B: Biomedical Sciences and Applications* **377**, 350-355 (1986).
40. Mills MH, Finlay DC, Haddad PR. Determination of melatonin and monoamines in rat pineal using reversed-phase ion-interaction chromatography with fluorescence detection. *Journal of Chromatography B: Biomedical Sciences and Applications* **564**, 93-102 (1991).
41. Peniston-Bird J, Di W, Street CA, Kadva A, Stalteri MA, Silman RE. HPLC assay of melatonin in plasma with fluorescence detection. *Clinical chemistry* **39**, 2242-2247 (1993).
42. Chin JL. Determination of six indolic compounds, including melatonin, in rat pineal using high-performance liquid chromatography with serial fluorimetric—electrochemical detection. *Journal of Chromatography B: Biomedical Sciences and Applications* **528**, 111-121 (1990).
43. Vieira R, Míguez J, Lema M, Aldegunde M. Pineal and plasma melatonin as determined by high-performance liquid chromatography with electrochemical detection. *Analytical biochemistry* **205**:300-305 (1992).
44. Chanut E, Nguyen-Legros J, Versaux-Botteri C, Trouvin J-H, Launay J-M. Determination of melatonin in rat pineal, plasma and retina by high-performance liquid chromatography with electrochemical detection. *Journal of Chromatography B: Biomedical Sciences and Applications* **709**, 11-8 (1998).
45. Musijowski J, Poboży E, Trojanowicz M. On-line preconcentration techniques in determination of melatonin and its precursors/metabolites using micellar electrokinetic chromatography. *Journal of chromatography A* **1104**, 337-345 (2006).
46. Wilson BW, Snedden W, Silman R, Smith I, Mullen P. A gas chromatography-mass spectrometry method for the quantitative analysis of melatonin in plasma and cerebrospinal fluid. *Analytical biochemistry* 1977;**81**:283-91.
47. Skene D, Leone R, Young I, Silman R. The assessment of a plasma melatonin assay using gas chromatography negative ion chemical ionization mass spectrometry. *Biomedical mass spectrometry* **10**, 655-659 (1983).
48. Lee C, Esnaud H. Determination of melatonin in blood plasma, using capillary gas chromatography and electron impact medium-resolution mass spectrometry. *Biomedical & environmental mass spectrometry* **15**, 249-252 (1988).
49. Fournillan J, Gobin P, Faye B, Girault J. A highly sensitive assay of melatonin at the femtogram level in human plasma by gas chromatography/negative ion chemical ionization mass spectrometry. *Biological mass spectrometry* **23**, 499-509 (1994).
50. Simonin G, Bru L, Lelievre E, Jeannot J-P, Bromet N, Walther B. Determination of melatonin in biological fluids in the presence of the melatonin agonist S 20098: comparison of immunological techniques and GC-MS methods. *Journal of pharmaceutical and biomedical analysis* **21**, 591-601 (1999).

51. Kocadağlı T, Yılmaz C, Gökmen V. Determination of melatonin and its isomer in foods by liquid chromatography tandem mass spectrometry. *Food chemistry* **153**, 151-156 (2014).
52. Severcan F, Sahin I, Kazancı N. Melatonin strongly interacts with zwitterionic model membranes—evidence from Fourier transform infrared spectroscopy and differential scanning calorimetry. *Biochimica et Biophysica Acta (BBA)-Biomembranes* **1668**, 215-222 (2005).
53. Kaczmarek M. Lanthanide ions (III) as sensitizers of melatonin oxidation in reaction mixtures providing reactive species of oxygen and nitrogen. *Journal of Luminescence* **162**, 31-35 (2015).
54. Bazrgar M, Goudarzi I, Lashkarbolouki T, Salmani ME. Melatonin ameliorates oxidative damage induced by maternal lead exposure in rat pups. *Physiology & behavior* **151**, 178-188 (2015).
55. Li X, Wang S. Binding of glutathione and melatonin to human serum albumin: A comparative study. *Colloids and Surfaces B: Biointerfaces* **125**, 96-103 (2015).
56. Zephy D, Ahmad J. Type 2 diabetes mellitus: role of melatonin and oxidative stress. *Diabetes & Metabolic Syndrome: Clinical Research & Reviews* **9**, 127-131 (2015).
57. Hafner A, Lovrić J, Romić MD, Juretić M, Pepić I, Cetina-Čižmek B. Evaluation of cationic nanosystems with melatonin using an eye-related bioavailability prediction model. *European Journal of Pharmaceutical Sciences* **75**, 142-150 (2015).
58. de la Fuente Revenga M, Herrera-Arozamena C, Fernández-Sáez N, Barco G, García-Orue I, Sugden D. New coumarin-based fluorescent melatonin ligands. Design, synthesis and pharmacological characterization. *European journal of medicinal chemistry* **103**, 370-373 (2015).
59. Cerezo AB, Leal Á, Álvarez-Fernández MA, Hornedo-Ortega R, Troncoso AM, García-Parrilla MC. Quality control and determination of melatonin in food supplements. *Journal of food composition and Analysis* **45**, 80-86 (2016).
60. Oliver A, Stainton J, Taylor P. A simple filter-paper disc method for determining the sensitivity of Myco. tuberculosis. *Journal of clinical pathology* **12**, 444 (1959).
61. Gupta R, Saxena R, Chaturvedi P, Viridi J. Chitinase production by *Streptomyces viridificans*: its potential in fungal cell wall lysis. *Journal of Applied Bacteriology* **78**, 378-383 (1995).
62. Geary WJ. The use of conductivity measurements in organic solvents for the characterisation of coordination compounds. *Coordination Chemistry Reviews* **7**, 81-122 (1971).
63. Gupta SP, Bhati M, Jhajharia K, Patel H, Paliwal A, Franklin S. Evaluation of antimicrobial and antifungal efficacy of inter appointment intracanal medicaments against *Enterococcus* and *Candida albicans*: an in vitro study. *Journal of international oral health: JIOH* **7**, 97 (2015).
64. Geary W.J. The use of conductivity measurements in organic solvents for the characterisation of coordination compounds. *Coordination Chemistry Reviews* **7**(1), 81-122 (1971).
65. Fazakerley G, Linder PW, Nassimbeni L. Complexation of copper (II) by chloramphenicol. *Inorganic and Nuclear Chemistry Letters* **9**, 1069-1072 (1973).
66. Nakamoto K. Infrared spectra of inorganic and coordination compounds. (1970).
67. Brisdon A. Kazuo Nakamoto Infrared and Raman Spectra of Inorganic and Coordination Compounds, Part B, Applications in Coordination, Organometallic, and Bioinorganic Chemistry, 6th edn Wiley, 2009, 424 pp.(hardback) ISBN 978-0-471-74493-1. *Applied Organometallic Chemistry* **24**, 489- (2010).
68. [47] Cotton FA, Goodgame DM, Goodgame M. Absorption spectra and electronic structures of some tetrahedral manganese (II) complexes. *Journal of the American Chemical Society* **84**, 167-172 (1962).
69. Figgis B.N. Introduction to Ligand Fields. *Interscience Publishers, John Wiley and Sons, New York*, **285** (1967).
70. Gliemann G. ABP Lever: Inorganic Electronic Spectroscopy, Vol. 33 aus: Studies in Physical and Theoretical Chemistry, Elsevier, Amsterdam, Oxford, New York, Tokio 1984. 863 Seiten, 50. *Berichte der Bunsengesellschaft für physikalische Chemie* **89**, 99-100 (1985).
71. Rabinovich D. Advanced Inorganic Chemistry, (Cotton, FA; Wilkinson, G.; Murillo, CA; Bochmann, M.). ACS Publications (2000).
72. Earnshaw A. Introduction to magnetochemistry:
- Egypt. J. Chem.* **Vol. 63**, No. 4 (2020)

Elsevier (2013).

73. Sacconi L. Electronic structure and stereochemistry of Ni (II). *Transition Metal Chemistry* (1968).
74. Cullity B. Elements of x-ray diffraction second edition. by Addison-Wesley Publishing Co, Inc, Massachusetts 99-106 (1978).
75. Flynn JH, Wall LA. General treatment of the thermogravimetry of polymers. *J Res Nat Bur Stand* **70**, 487-523 (1966).